Wind and Structures, Vol. 9, No. 2 (2006) 125-146
DOI: http://dx.doi.org/10.12989/was.2006.9.2.125

Flutter analysis of Stonecutters Bridge

Michael C. H. Hui[†1),2)] and Q. S. Ding[‡2)]

[1)]*Major Works Project Management Office, Highways Department, 6/F, Ho Man Tin Government Offices, 88 Chung Hau Street, Kowloon, Hong Kong, China*
[2)]*State Key Laboratory for Disaster Reduction in Civil Engineering and Department of Bridge Engineering, Tongji University, Shanghai 200092, China*

Y. L. Xu[‡†]

Department of Civil and Structural Engineering, The Hong Kong Polytechnic University, Hung Hom, Kowloon, Hong Kong, China

(Received April 7, Revised November 15, 2005 , Accepted February 2, 2006)

Abstract. Stonecutters Bridge of Hong Kong is a cable-stayed bridge with two single-column pylons each 298 m high and an aerodynamic twin deck. The total length of the bridge is 1596 m with a main span of 1018 m. The top 118 m of the tower will comprise structural steel and concrete composite while the bottom part will be of reinforced concrete. The bridge deck at the central span will be of steel whilst the side spans will be of concrete. Stonecutters Bridge has adopted a twin-girder deck design with a wide clear separation of 14.3 m between the two longitudinal girders. Although a number of studies have been conducted to investigate the aerodynamic performance of twin-girder deck, the actual real life application of this type of deck is extremely limited. This therefore triggered the need for conducting the present studies, the main objective of which is to investigate the performance of Stonecutters Bridge against flutter at its in-service stage as well as during construction. Based on the flutter derivatives obtained from the 1:80 scale rigid section model experiment, flutter analysis was carried out using 3-D finite element based single parameter searching method developed by the second author of this paper. A total of 6 finite element models of the bridge covering the in-service stage as well as 5 construction stages were established. The dynamic characteristics of the bridge associated with these stages were computed and applied in the analyses. Apart from the critical wind speeds for the onset of flutter, the dominant modes of vibration participating in the flutter vibration were also identified. The results indicate that the bridge will be stable against flutter at its in-service stage as well as during construction at wind speeds much higher than the verification wind speed of 95 m/s (1-minute mean).

Keywords: Stonecutters Bridge; flutter; multi-mode and single parameter searching.

1. Introduction

Stonecutters Bridge being built in Hong Kong will be a cable-stayed bridge having a main span of

† Chief Engineer, Corresponding Author, E-mail: mchhui@graduate.hku.hk
‡ Research Associate
‡† Professor

1018 m. A bridge of this span will be subject to a variety of wind-induced vibration problems. This, coupled with the extreme typhoon wind climate in Hong Kong necessitates, as part of the design procedure, extensive aerodynamic investigations. Stonecutters Bridge has adopted a twin-girder deck design with a wide clear separation of 14.3 m between the two longitudinal girders. A number of studies have been conducted to look at the flutter problem related to this kind of deck. Sato, *et al.* (2000) studied a combined 1-box and 2-box girder section and found from the multi-mode flutter analyses to a suspension bridge having a main span of 2500 m that the flutter onset velocity in the 2-box and 1-box combined girder can be notably higher than that in the 1-box combined girder. Ogawa, *et al.* (2002) found that a slot at the centre of a girder would be effective in improving aerodynamic stability. Matsumoto, *et al.* (2004) looked at the flutter characteristics of long span bridges with separated two box girders from the point of view of unsteady pressure distribution on bridge deck surface during heaving/torsional vibration related to the aerodynamic derivatives. Flutter is a catastrophic phenomenon and should be avoided in the design of long span cable supported bridges. As Stonecutters Bridge will be one of the longest span cable stayed bridges in the world when completed in 2008, flutter analysis was carried out as part of the aerodynamic investigation.

For a long time, wind induced oscillations have been a poorly understood phenomenon, difficult to predict and believed to be important in long spans and flexible structures mainly. Occasionally, a static allowance was made to cater for dynamic effects, with no real understanding of their cause. The failure of the Tacoma Narrows Bridge in 1940 laid a significant milestone in the history of bridge aerodynamics in the development of quantitative assessment of wind effects, comprising a combination of experimental, analytical and numerical approaches. With the advances of computer technology in the late 80's/early 90's, many researchers became able to develop analytical approaches which involve substantial computational effort. Multimode flutter analysis is one of the approaches that has attracted the attention of academia. This method converts the large physical system of a structure into a generalised system containing only a few degrees of freedom associated with the first several low-frequency natural modes of the structure. Substantial contributions were made by researchers on analytical investigations related to the flutter problems of long-span bridges (e.g. Bleich 1948, Scanlan, *et al.* 1978, 1987, 1990 and 1993, Lin 1979, Xie and Xiang 1985, Miyata, *et al.* 1988 and 1994, Agar 1989, Namini and Albrecht 1992, Chen 1994, Jain, *et al.* 1996, Xiang, *et al.* 1996, Dung, *et al.* 1998, Diana, *et al.* 1999, Boonyapinyo, *et al.* 1999, Ge, *et al.* 2000, Chen, *et al.* 2000a, 2000b and 2003). The following discussions briefly summarize the gist of the work of these pioneers: Scanlan (1978) proposed a basic theory for multimode flutter analysis. He also suggested a mode-by-mode approach on the basis that practical flutter problems of long-span bridges are mostly damping-driven flutter and are dominated by the action of a single mode. Lin (1979) modelled mathematically the effect of turbulence on flutter instability with random parametric excitation analysis and found that the turbulent component of wind may reduce flutter velocity in some cases. Xie and Xiang (1985) employed a planar model of unsteady aerodynamic forces and presented a state-space method for multimode flutter problems. Agar (1989) converted the flutter motion equation into the eigenvalue problem of a real unsymmetric matrix, but the flutter analysis requires a two-parameter searching process. Namini and Albrecht (1992) proposed the pK-F method for multimode flutter problems. The method is to solve nonlinear equations by iteration and can provide the information about variations of structural dynamic behaviors with the wind speed. Chen (1994) transferred the flutter problem into a complex generalized eigenvalue problem and proposed the M-S method that did not require iteration in non-damping situations. Jain (1996) also presented a complex method for the coupled flutter problem, involving the solving of the real

and imaginary parts of the characteristic polynomial. Dung, *et al*. (1998) suggested a direct flutter analysis and solved the characteristic equation by the mode tracing method. Chen, *et al*. (2000a) expressed the aerodynamic forces of a bridge deck by rational functions whose coefficients were derived from flutter derivatives. They analyzed the flutter problem by the state-space method. The majority of these methods are mainly based on the modal coordinates of the structure, so the computations are efficient and each method has its own advantages. However, one characteristic about these methods is that the participating modes in the flutter motion must be chosen beforehand and this would necessitate much personal participation in the flutter analysis process.

This study aims to investigate the performance of Stonecutters Bridge against flutter at its in-service stage as well as during construction based on the flutter derivatives obtained from the 1:80 scale rigid section model experiment and the 3D finite element based single parameter searching

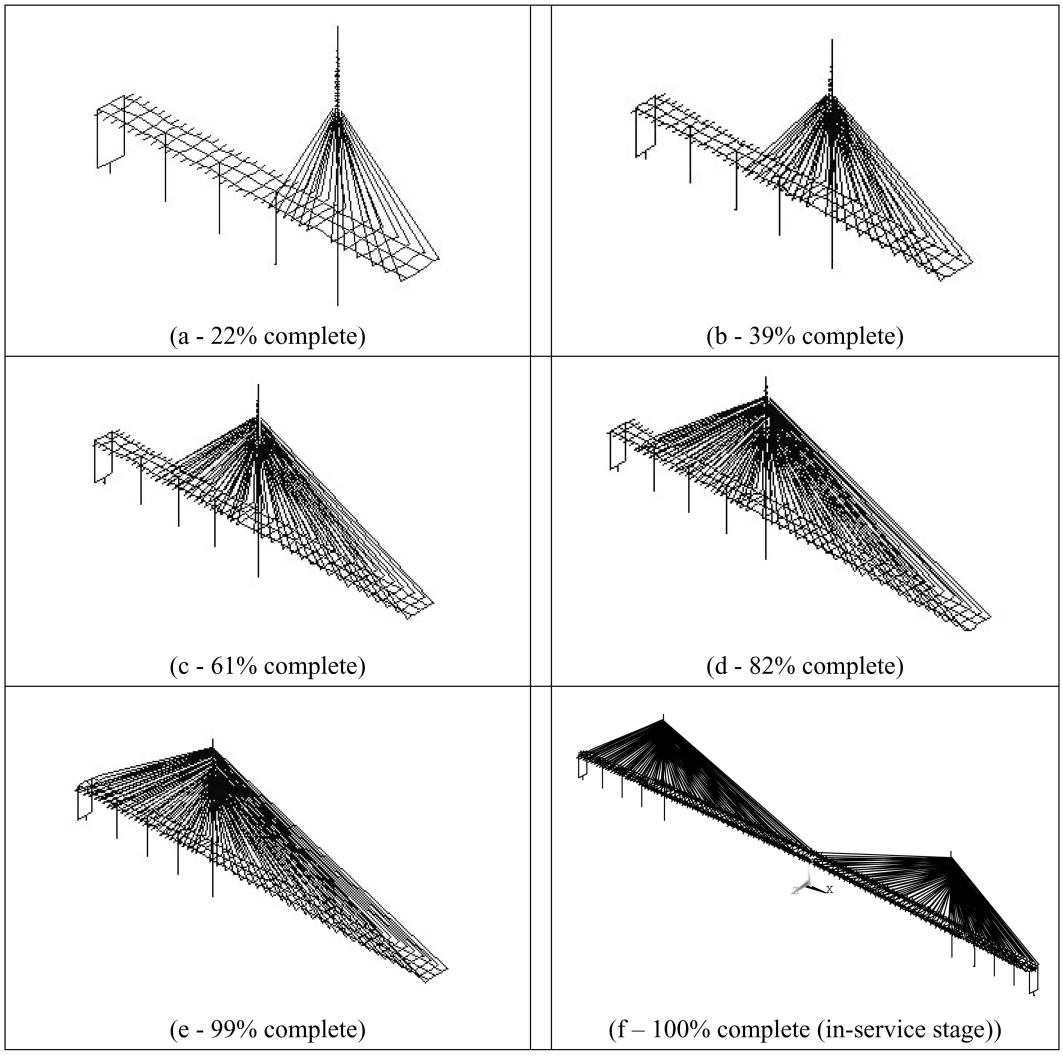

Fig. 1 Finite element model of Stonecutters Bridge

method developed by the second author of this paper (Ding, *et al*. 2001). A total of 6 finite element models of the bridge were established for the completion stage as well as for the 5 construction stages representing 22%, 39%, 61%, 82% and 99% completion of half of the main span length of the bridge (see Fig. 1). The dynamic characteristics of the bridge associated with these stages were computed and applied in the analyses. Apart from the critical wind speeds for the onset of flutter, the dominant modes of vibration participating in the flutter vibration were also identified. The major findings of the investigation results are presented in this paper.

2. Multimode and single parameter searching approach

2.1. Equation of motion

Assuming that flutter of a long span cable supported bridge occurs under a smooth flow condition, buffeting forces will therefore have no influence on the aerodynamic stability and the predominant forces acting on a bridge will be the self-excited forces. The governing equation of motion can be written as:-

$$\mathbf{M}\ddot{\mathbf{X}} + \mathbf{C}\dot{\mathbf{X}} + \mathbf{K}\mathbf{X} = \mathbf{F}_{\mathbf{se}} \tag{1}$$

where **M**, **C**, and **K** are the structural mass, damping, and stiffness matrix, respectively; **X**, $\dot{\mathbf{X}}$, $\ddot{\mathbf{X}}$ are the nodal displacement, velocity, and acceleration vector; respectively; $\mathbf{F}_{\mathbf{se}}$ indicates the nodal equivalent self-excited force vector.

2.2. Self-excited forces and multi-mode flutter analysis

The self-excited vertical and lateral forces and self-excited moment acting on the bridge deck per unit length are expressed often in terms of Scanlan's format as follows:

$$L_{se}(t) = \frac{1}{2}\rho\overline{U}^2(2B)\left(KH_1^*\frac{\dot{h}}{\overline{U}} + KH_2^*\frac{B\dot{\alpha}}{\overline{U}} + K^2H_3^*\alpha + K^2H_4^*\frac{h}{B} + KH_5^*\frac{\dot{p}}{\overline{U}} + K^2H_6^*\frac{p}{B}\right) \tag{2a}$$

$$D_{se}(t) = \frac{1}{2}\rho\overline{U}^2(2B)\left(KP_1^*\frac{\dot{p}}{\overline{U}} + KP_2^*\frac{B\dot{\alpha}}{\overline{U}} + K^2P_3^*\alpha + K^2P_4^*\frac{p}{B} + KP_5^*\frac{\dot{h}}{\overline{U}} + K^2P_6^*\frac{h}{B}\right) \tag{2b}$$

$$M_{se}(t) = \frac{1}{2}\rho\overline{U}^2(2B^2)\left(KA_1^*\frac{\dot{h}}{\overline{U}} + KA_2^*\frac{B\dot{\alpha}}{\overline{U}} + K^2A_3^*\alpha + K^2A_4^*\frac{h}{B} + KA_5^*\frac{\dot{p}}{\overline{U}} + K^2A_6^*\frac{p}{B}\right) \tag{2c}$$

where ρ is the air density; $\overline{U}$ is the mean wind velocity; B is the bridge deck width; $K = \omega B/\overline{U}$ is the reduced frequency; ω is the circular frequency of vibration; h, p, and α are the vertical, lateral, and torsional displacements of the bridge deck, respectively; the over-dot denotes the partial differentiation with respect to time t; and H_i^*, P_i^*, A_i^* $(i = 1\sim6)$ are the non-dimensional flutter derivatives.

Let $\mathbf{X} = \Phi\mathbf{q}e^{st}$, where Φ is the $n \times m$ matrix of mode shapes, given by the dynamic characteristics analysis; $\mathbf{q}$ is the m vector of generalized coordinates; and n is the total number of degrees of freedom. Denote the complex frequency $s = (-\xi + i)\omega$ (where ξ and ω are the damping ratio and circular frequency of the complex mode of vibration, respectively, and $i^2 = -1$). Considering the fact that the damping ratios of the system are small, the circular frequency of a complex mode is

approximately given by $\omega = -is$. Substituting this relationship into the governing equation of motion and express it in the state-space format, the complex mode analysis of the system will finally be converted into a standard eigenvalue problem (Ding, *et al.* 2001):

$$\mathbf{AY} = s\mathbf{Y} \tag{3}$$

where $\mathbf{Y} = \begin{Bmatrix} \mathbf{q} \\ s\mathbf{q} \end{Bmatrix}$ and the characteristic matrix $\mathbf{A}$ is a 2 m × 2 m complex matrix and a function of reduced frequency K only. Thus, the above equation can be solved for only two variables, s and K. For a given K, standard linear eigensolvers are available to find the 2 m sets of eigenvalues s and the corresponding eigenvectors $\mathbf{Y}$ from the above equation.

$$s = (-\xi + i)\omega, \quad \mathbf{q} = \mathbf{a} + \mathbf{b}i, \tag{4}$$

The m eigenvalues with positive imaginary part are the complex frequencies of the system, and the upper half vector $\mathbf{q}$ in the corresponding eigenvector $\mathbf{Y}$ is the complex mode shape of the system. In a prescribed complex mode shape, the magnitude and phase of the kth natural mode are given as

$$|q_k| = \sqrt{a_k^2 + b_k^2}, \quad \varphi_k = \tan^{-1}(b_k / a_k) \tag{5}$$

If the damping ratios of all complex modes are positive, the system is stable; if at least one damping ratio is equal to zero, the system is neutrally stable; if at least one damping ratio is negative, the system is unstable. Therefore, the flutter analysis described above is able to find the critical state through searching the reduced frequency K. The corresponding circular frequency is the flutter circular frequency ω_f and the critical wind speed U_{cr} is then equal to $B\omega_f/K$. At the critical wind speed, the generalized modal coordinate vector $\mathbf{q}(t)$ and the nodal displacement vector of the bridge can be expressed as

$$\mathbf{q}(t) = \{|q_i|\sin(\omega_f t + \varphi_i)\} \tag{6}$$

$$\mathbf{X}(t) = \sum_{i=1}^{m} \phi_i |q_i| \sin(\omega_f t + \varphi_i) = \mathbf{X}_0 \sin(\omega_f t + \overline{\varphi}) \tag{7}$$

where ϕ_i is the ith natural mode shape; ω_f is the flutter circular frequency; $\mathbf{X}_0$ and $\overline{\varphi}$ are the amplitude and phase of $\mathbf{X}(t)$; m is the number of participating modes. It is clear that the coupled flutter motion is three-dimensional and that the phase shift exists among mode components.

The total energy in the characteristic motion (flutter motion) of the bridge at the lowest critical wind speed is

$$E = \frac{1}{2}\{\dot{\mathbf{X}}_{\max}\}^T \mathbf{M} \{\dot{\mathbf{X}}_{\max}\} = \frac{1}{2}\omega_f^2 \sum_{i=1}^{m} |q_i|^2 \tag{8}$$

The energy in the ith natural mode of vibration of the bridge is expressed as

$$E_i = \frac{1}{2}\omega_f^2 |q_i|^2 \tag{9}$$

The ratio of the ith modal energy over the total energy E_i / E is defined as the modal energy ratio

e_i. Clearly, the modal energy ratio provides a uniform measurement to the contribution of a particular vibration mode to the flutter instability of the whole bridge.

3. Dynamic characteristics of Stonecutters Bridge

Stonecutters Bridge is a cable stayed bridge with a total length of 1596 m and a steel main span of 1018 m. The concrete back spans are comprised of four spans of 69.25 m, 70 m, 70 m and 79.75 m, respectively. The bridge towers are 298 m high mono columns. The towers are designed as reinforced concrete structure up to level +175 m and as a steel concrete composite from +175 m to +293 m. The top 5m is non-structural and contains architectural lighting and maintenance equipment. The bridge deck over the central 1117.5 m is designed as twin girder steel structure supported by stay cables every 18 m at the outer edges of the deck. At the location of the stay cables, the two longitudinal deck girders are interconnected by cross girders. The transition in the deck from steel to concrete is located 49.75 m into the back spans. The concrete deck is a twin girder box structure as the steel deck and is designed with external unbonded longitudinal pre-stressing and bonded internal transverse pre-stressing at the cross girders. The piers in the back span are all connected monolithically to the bridge deck. The three intermediate piers are mono column piers, while the last pier towards the approaching viaduct is a twin pier structure. The bridge deck is supported by stay cables in the main span and by stay cables and piers in the back span. Globally speaking, the bridge is supported laterally at the towers on bearings and on the back span piers. Longitudinally, the bridge deck and towers are interconnected by hydraulic buffers that will restrain fast movements such as dynamic part of the wind and from the seismic actions, and will allow slow movements due to temperature variations.

Stonecutters Bridge Global models were used for assessing the global flutter stability of the bridge. No local or semi-local models of the bridge were involved in this study. As the exact construction sequence was not known at the time of study, some assumptions and/or simplifications have to be made in the modeling. Temporary supporting systems used at the construction stage are not taken into consideration in the finite element modeling and flutter analysis. Only three-dimensional beam elements and truss elements are used to model the bridge components. The bridge deck, tower, and piers are all modelled using the beam elements with 6 degrees of freedom in each node while the stay cables are modelled using spatial truss element with 3 degrees of freedom at each end of the element. In order to simplify the calculation and to focus on the global flutter stability of the bridge, each stay cable is modeled as a single truss element. This simplification has negligible effect on the global dynamic characteristics of the bridge as the characteristics of the completed bridge using 10 truss elements for stay cables were checked to be similar to that using 1 truss element. The effect of pre-stressing in the concrete deck is considered insignificant for predicting the global dynamic characteristics of the bridge. Temporary loads on the bridge deck at the construction stage were assumed to be that as shown in Fig. 2.

For dynamic characteristics analyses of very long-span cable supported bridges, the geometric non-linearity due to tension forces in the cables and axial forces in the bridge deck and towers are considered in the modal (eigenvalue) analysis. The natural frequencies of the bridge can be found from the following determinant:-

$$|[K] - \omega^2[M]| = 0 \tag{10}$$

where $[K]$ and $[M]$ are the total stiffness and mass matrix of the bridge at the construction stage;

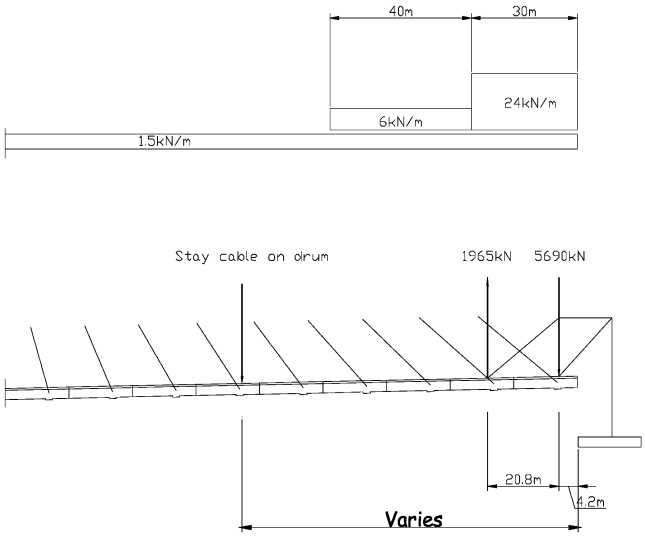

Fig. 2 Temporary loads on the bridge deck at the construction stage

and ω is the circular frequency. It is noted that the stiffness matrix $[K]$ is a combination of the structural stiffness matrix and the geometric stiffness matrix whereas the geometric stiffness matrix is obtained through a static analysis of the 3-D finite element model of the bridge for each construction stage.

3.1. Dynamic characteristics of the completed bridge

In the 3-D global finite element model of the bridge, two longitudinal beams are used to represent the two longitudinal girders in the bridge deck (see Fig. 1f). The centre of each longitudinal beam is located at the gravity centre of the corresponding longitudinal girder. Three-dimensional beam elements with six-degree-of-freedom at each node are used to model the two longitudinal beams. Shear deformations are taken into consideration. Each longitudinal beam is divided into 124 beam elements with a total of 125 nodes. A total of 62 steel cross girders are used to connect the two longitudinal steel girders. Each steel cross girder is modelled as a cross beam of a typical length of 18.5 m. The end of each cross beam is then connected to the longitudinal beams through rigid arms. There are a total of 10 intermediate concrete cross girders in one side span to connect the two longitudinal concrete girders, each of which is modelled by one cross beam with a certain length varying along the bridge axis. When the total mass matrix and the total stiffness matrix are assembled, the modal analysis can be performed according to Eq. (10) using the subspace iteration approach.

The first 50 natural frequencies and periods were analysed. As higher modes would not participate in the bridge flutter, only the first 15 modes are presented in Table 1 together with their nature.

The salient points to note from the modal analysis of the completed Stonecutters Bridge can be summarized as follows:

- The first 15 natural frequencies of the complete bridge range from 0.145 Hz to 0.525 Hz.
- The lowest natural frequency of 0.145 Hz corresponds to the first horizontal vibration mode in

Table 1 Dynamic characteristics of the complete Stonecutters Bridge (100%)

Mode No.	Natural frequency (Hz)	Period (sec)	Mode shape description
1	0.145	6.875	1. symmetric horizontal, deck
2	0.190	5.260	1. asymmetric horizontal, towers
3	0.197	5.073	1. symmetric horizontal, towers
4	0.201	4.968	1. symmetric vertical, deck
5	0.246	4.072	1. asymmetric vertical, deck
6	0.302	3.311	2. asymmetric vertical, deck
7	0.311	3.217	2. symmetric vertical, deck
8	0.361	2.772	1. asymmetric horizontal, deck
9	0.376	2.660	3. asymmetric vertical, deck
10	0.422	2.372	3. symmetric vertical, deck
11	0.425	2.354	1. symmetric torsional, deck
12	0.444	2.250	Horizontal, deck and piers, west side span
13	0.452	2.214	Horizontal, deck and piers, east side span
14	0.490	2.040	4. asymmetric vertical, deck
15	0.525	1.903	2. symmetric horizontal, towers

which the motion of the bridge deck is almost in symmetry in the main span. The second horizontal vibration mode dominated by the bridge deck is almost asymmetric in the main span at a natural frequency of 0.361 Hz. The first two natural frequencies in the horizontal vibration modes dominated by the bridge deck are well separated.

- Following the first horizontal mode of the bridge deck is the two horizontal vibration modes dominated by the bridge towers. At the natural frequency of 0.190 Hz, two towers move in opposite directions whereas at the natural frequency of 0.197 Hz, the two towers move in the same direction.
- The first vertical vibration mode dominated by the bridge deck is almost symmetrical in the main span at a natural frequency of 0.201 Hz. The second vertical vibration mode dominated by the bridge deck is almost asymmetrical in the main span at a natural frequency of 0.246 Hz. The first two natural frequencies in the vertical modes of vibration are relatively close.
- The first torsional vibration mode dominated by the bridge deck is almost symmetrical in the main span at a natural frequency of 0.425 Hz while the second one (mode no. 18) is almost asymmetrical in the main span at a natural frequency of 0.591 Hz.
- The motion of bridge towers is often involved in the horizontal modes or the vertical modes dominated by the bridge deck.

3.2. Dynamic characteristics of the bridge at the 99% completion stage

For the construction stage of the Stonecutters Bridge at 99% completion, the length of the bridge deck in the main span on the west side is 506.35 m and 28 sets of stay cables are installed and tensioned on each side of the tower. The total length of each longitudinal steel deck is 556.1 m and it is modelled with 33 beam elements. There are 31 steel cross girders connecting the two longitudinal steel girders.

Table 2 Dynamic characteristics of the Stonecutters Bridge with 99% completion

Mode No.	Natural frequency (Hz)	Period (sec)	Mode shape description
1	0.116	8.635	1. Horizontal, deck
2	0.194	5.158	1. Horizontal, tower
3	0.212	4.728	1. Vertical, deck
4	0.296	3.378	2. Vertical, deck
5	0.329	3.037	3. Vertical, deck
6	0.443	2.260	4. Vertical, deck
7	0.454	2.204	Torsional and horizontal, deck
8	0.456	2.191	Torsional and horizontal, deck & horizontal tower
9	0.535	1.869	Torsional and horizontal, deck & horizontal tower
10	0.582	1.718	Vertical, deck
11	0.677	1.476	Horizontal, tower & horizontal deck
12	0.739	1.353	Vertical, deck
13	0.805	1.243	Torsional, deck
14	0.906	1.104	Vertical, deck
15	0.931	1.074	Horizontal, deck & horizontal, tower

The first 30 natural frequencies and mode shapes were analysed for the bridge at 99% completion. Table 2 lists the first 15 natural frequencies and periods and provides a general description of the nature of mode shapes.

The salient points from the modal analysis of Stonecutters Bridge at 99% completion can be summarized as follows:

- The first 15 natural frequencies of the bridge at 99% completion range from 0.116 Hz to 0.931 Hz.
- The lowest natural frequency of 0.116 Hz corresponds to the first horizontal vibration mode dominated by the bridge deck, which is much lower than that at the 100% completion stage after the closure of the main span.
- The first horizontal vibration mode of the bridge tower follows the first horizontal vibration mode dominated by the bridge deck and at a natural frequency of 0.194 Hz, which is similar to that at 100% completion.
- The first vertical vibration mode dominated by the bridge deck occurs at a natural frequency of 0.212 Hz, which again is similar to that at 100% completion.
- The first torsional vibration mode dominated by the bridge deck occurs at a natural frequency of 0.454 Hz, which again is similar to that at 100% completion. This mode is coupled with the horizontal motion of the bridge deck.
- The vertical modes of vibration of the bridge deck occur very often and closely spaced.

3.3. Dynamic characteristics of the bridge at the 82% completion stage

For the construction stage of the Stonecutters Bridge at 82% completion, the length of the bridge deck in the main span on the west side is 416.35 m and 23 sets of stay cables are installed and

Table 3 Dynamic characteristics of the Stonecutters Bridge at 82% completion

Mode No.	Natural frequency (Hz)	Period (sec)	Mode shape description
1	0.157	6.378	1. Horizontal, deck
2	0.201	4.984	1. Horizontal, tower
3	0.247	4.057	1. Vertical, deck
4	0.323	3.099	Longitudinal, tower & vertical, deck
5	0.398	2.510	2. Vertical, deck
6	0.456	2.192	Horizontal, tower & horizontal, deck
7	0.541	1.849	Torsional and horizontal, deck
8	0.567	1.764	Vertical, deck
9	0.596	1.677	Torsional and horizontal, deck
10	0.744	1.343	Vertical, deck
11	0.839	1.192	Horizontal, tower & horizontal and torsional, deck
12	0.922	1.085	Vertical, deck
13	0.938	1.066	Horizontal, tower & horizontal and torsional, deck
14	0.987	1.013	Torsional, deck
15	0.992	1.008	Longitudinal, tower & vertical, deck

tensioned on each side of the bridge tower. The total length of each longitudinal steel deck is 466.1 m and it is modelled with 28 beam elements. There are 26 steel cross girders connecting the two longitudinal steel girders.

The first 30 natural frequencies and mode shapes were analysed for the bridge at 82% completion. Table 3 lists the first 15 natural frequencies and periods and provides a general description of the nature of mode shapes.

The salient points to note from the modal analysis of Stonecutters Bridge at 82% completion can be summarized as follows:

- The first 15 natural frequencies of the bridge at 82% completion range from 0.157 Hz to 0.992 Hz.
- The lowest natural frequency of 0.157 Hz corresponds to the first horizontal vibration mode dominated by the bridge deck, which is similar to that at 100% completion but much higher than that at 99% completion.
- As for the 100% and 99% completion, the first horizontal mode of the bridge tower occurs after the first horizontal vibration mode of the bridge and at a similar natural frequency of 0.201 Hz.
- The first vertical vibration mode dominated by the bridge deck occurs at a natural frequency of 0.247 Hz, which is comparable to 0.201 Hz and 0.212 Hz at 100% and 99% completion, respectively.
- The first torsional vibration mode dominated by the bridge deck occurs at a natural frequency of 0.541 Hz, which is comparable to 0.425 Hz and 0.454 Hz at 100% and 99% completion, respectively.
- The coupling between the torsional and horizontal motions of the bridge deck and the horizontal motion of the bridge tower is clearly observed.

3.4. Dynamic characteristics of the bridge at the 61% completion stage

For the construction stage of the Stonecutters Bridge at 61% completion, the length of the bridge

Table 4 Dynamic characteristics of the Stonecutters Bridge at 61% completion

Mode No.	Natural frequency (Hz)	Period (sec)	Mode shape description
1	0.190	5.251	1. Horizontal, tower
2	0.261	3.831	1. Horizontal, deck
3	0.277	3.611	1. Vertical, deck
4	0.354	2.823	Longitudinal, tower & vertical, deck
5	0.452	2.212	Horizontal, tower & horizontal deck
6	0.530	1.886	Vertical, deck
7	0.608	1.645	Horizontal, tower & horizontal deck
8	0.724	1.382	1. Torsional, deck
9	0.756	1.323	Longitudinal, tower
10	0.773	1.293	Vertical, deck
11	0.948	1.055	Horizontal, tower & horizontal deck
12	0.998	1.002	Vertical, deck
13	1.074	0.931	Vertical, deck & longitudinal, tower
14	1.124	0.889	Horizontal and torsional, deck
15	1.188	0.842	Vertical, deck

deck in the main span on the west side is 308.35 m and 17 sets of stay cables are installed and tensioned on each side of the tower. The total length of each longitudinal steel deck is 358.1 m and it is modelled with 22 beam elements. There are 20 steel cross girders connecting the two longitudinal steel girders.

The first 30 natural frequencies and mode shapes were analysed for the bridge at 61% completion. Table 4 lists the first 15 natural frequencies and periods and provides a general description of the nature of mode shapes.

The salient points to note from the modal analysis of the Stonecutters Bridge at 61% completion can be summarized as follows:

- The first 15 natural frequencies of the bridge at 61% completion range from 0.190 Hz to 1.188 Hz.
- The lowest natural frequency of 0.190 Hz corresponds to the first horizontal vibration mode of the bridge tower. This mode of vibration exists at various stages of construction discussed earlier with similar natural frequency.
- The first vibration mode dominated by the bridge deck is horizontal and occurs at a natural frequency of 0.261 Hz, which is much higher than that in the previous cases discussed.
- The first vertical vibration mode dominated by the bridge deck occurs at a natural frequency of 0.277 Hz, which is comparable to 0.201 Hz, 0.212 Hz and 0.247 Hz at 100%, 99% and 82% completion, respectively.
- The first torsional vibration mode dominated by the bridge deck occurs at a natural frequency of 0.724 Hz, which is much higher than that in the previous cases discussed.
- The vertical vibration mode of the bridge deck often couples with the longitudinal vibration mode of the bridge tower. The horizontal vibration mode of the bridge deck often couples with the horizontal vibration mode of the bridge tower.

3.5. Dynamic characteristics of the bridge at the 39% and 22% completion stages

For the construction stage of the Stonecutters Bridge at 39% completion, the length of the bridge deck in the main span on the west side is 200.35 m and 11 sets of stay cables are installed and tensioned on each side of the tower. The total length of each longitudinal steel deck is 250.1 m and it is modelled with 16 beam elements. There are 14 steel cross girders connecting the two longitudinal steel girders. The first vertical and torsional mode of vibration of the deck occur at a frequency of 0.261 Hz and 0.938 Hz respectively.

For the construction stage of the Stonecutters Bridge at 22% completion, the length of the bridge deck in the main span on the west side is 110.35 m and 6 sets of stay cables are installed and tensioned on each side of the tower. The total length of each longitudinal steel deck is 160.1 m and it is modelled with 11 beam elements. There are 9 steel cross girders connecting the two longitudinal steel girders. The first vertical and torsional mode of vibration of the deck occur at a frequency of 0.717 Hz and 1.036 Hz respectively.

As the vibration frequencies of the first vertical and torsional modes are very high, it can be expected that the critical wind speed for the onset of flutter associated with these 2 stages will be extremely high.

4. Flutter analysis and critical wind speed

4.1. General assumptions and information for flutter analysis

As discussed in Section 2, the aerodynamically coupled flutter analyses are carried out in the complex frequency domain. By using the modal coordinates of the bridge, the governing equation of the bridge for the flutter analysis was converted into a complex characteristic equation with only two variables. A single parameter searching method is then used to find the lowest critical wind speed without choosing participating modes beforehand. The major participating modes of vibration causing the flutter instability and the phase angles between the participating modes of vibration can also be found.

The flutter derivatives and the aerodynamic coefficients of the Stonecutters Bridge deck obtained from wind tunnel tests (DMI 2001) are for the complete bridge deck only. Only the flutter derivatives H_i^* and $A_i^*(i = 1\sim4)$ are available, and they are plotted in Fig. 3. The lift, drag, and moment coefficients of the deck section at zero degree of incidence are $C_D = 0.073$, $C_L = -0.155$, $C_M = -0.018$. The derivatives of these aerodynamic coefficients with respect to wind incidence at 0 degree of incidence are $dC_D/d\alpha = 0.0688$, $dC_L/d\alpha = 2.5097$, $dC_M/d\alpha = 0.5386$. Since the flutter derivatives related to the lateral motion of the bridge deck and the flutter derivatives H_5^*, H_6^*, A_5^*, H_6^* are not available, they are calculated based on the quasi-steady theory in terms of the aerodynamic coefficients. The aerodynamic parameters and the flutter derivatives mentioned above are assumed to be uniform along the bridge deck in the study.

$$P_1^* = -\frac{1}{K}C_D, \quad P_2^* = \frac{1}{2K}C_D', \quad P_3^* = \frac{1}{2K^2}C_D' \tag{11a}$$

$$P_5^* = \frac{1}{2K}C_D', \quad H_5^* = \frac{1}{K}C_L, \quad A_5^* = -\frac{1}{K}C_M \tag{11b}$$

$$P_4^* = P_6^* = H_6^* = A_6^* = 0 \tag{11c}$$

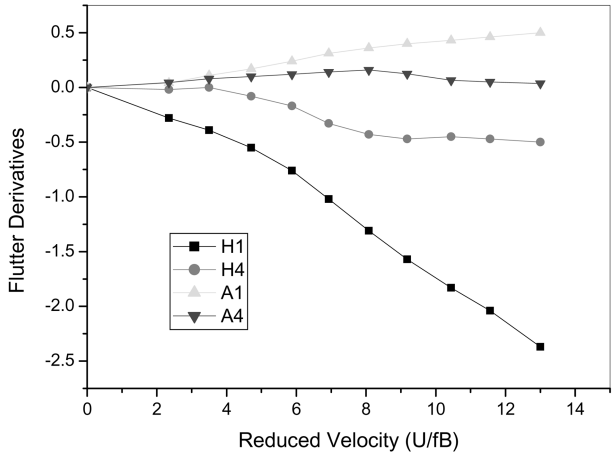

(a) Flutter derivatives H_1^*, H_4^*, A_1^*, A_4^*

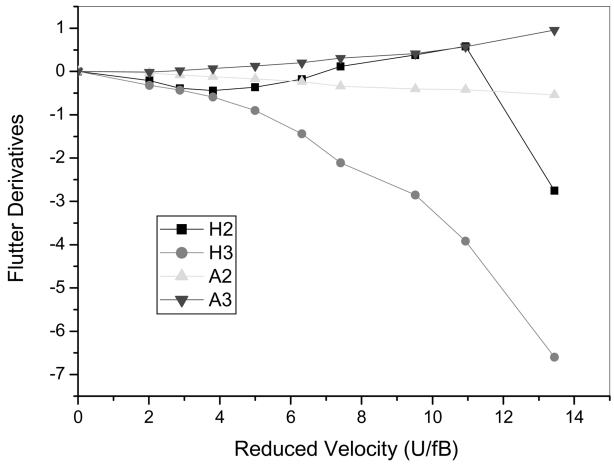

(b) Flutter derivatives H_2^*, H_3^*, A_2^*, A_3^*

Fig. 3 Flutter derivatives of the Stonecutters Bridge deck at the completion stage

It should be noted that the flutter derivatives and the aerodynamic coefficients of the Stonecutters bridge deck at the construction stages are not available and those at the completion stage are thus used. This assumption often results in conservative critical wind speeds because the parapets and service devices in the completed bridge deck are unfavorable in terms of flutter. The structural damping ratio is assumed to 0.0036 for all the modes of vibration of the bridge at both the completion and construction stages.

The effects of the towers, pier shafts, and stay cables on the flutter instability of the bridge as a whole are also taken into consideration for each construction stage and for the completion stage. The flutter derivatives for these bridge components are calculated based on the quasi-steady theory. Since the cross sections of the tower, pier shafts, and stay cables are basically circular, only the drag coefficients are needed to calculate the flutter derivatives required. The drag coefficients C_D for the bridge tower, pier shaft, and stay cable are taken as 1.2, 1.0, and 0.8, respectively.

4.2. Flutter analysis of the completed bridge

Since the method used for flutter analysis has no limit on the number of modes, the first 50 vibration modes of the completed bridge were employed as the participating modes for the flutter analysis of the completed bridge. The upper bound reduced velocity used in the measurement of flutter derivatives shown in Fig. 3 is extrapolated from 13.00 to 15.00 to facilitate the flutter analysis of the bridge at different construction stages. After the 3D characteristic equation for the flutter analysis of the completed bridge is established in the state-space format based on the information mentioned in section 4.1, the automatic searching method using the reduced frequency as a single searching parameter was applied to find the lowest critical wind speed. The lowest critical wind speed for the completed bridge was computed to be 230.4 m/s at a reduced velocity of 13.08 and a flutter frequency of 0.331 Hz (see Table 5). Such a high wind speed would unlikely occur in reality. Thus, the computed critical wind speed would be of theoretical interest only and it indicated no flutter instability problem for Stonecutters Bridge. It is noted that the reduced velocity corresponding to the lowest critical wind speed is very close to the upper bound reduced velocity for the flutter derivatives measured.

Corresponding to the lowest critical wind speed or the flutter frequency, a flutter eigenvector can be found. From the flutter eigenvector, one may observe the distribution of modal motion and modal energy over all the participating modes of vibration and the distribution of modal phase angle among all the participating modes of vibration. Then, from these distributions, the dominant modes of vibration causing the flutter instability can be identified. Figs. 4(a) to 4(c) display the distribution of relative modal amplitude, modal energy ratio, modal phase angle over the 50 participating modes of vibration, respectively. It is noted that vibration mode 4 (first symmetric vertical mode) and mode 11 (first symmetric torsional mode) are the two major participating modes dominating the flutter instability of the complete bridge with almost the same phase angle. Although the lateral vibration modes of the bridge deck also participate in the flutter motion, the degree of their participations is very small.

Apart from the modal information, Fig. 5 shows the relative amplitudes of the vertical, lateral, and torsional displacement responses (flutter motion) of the bridge deck along the bridge longitudinal axis at the lowest critical wind speed. It is noted again that the vertical and torsional vibrations dominate the flutter motion of the bridge deck.

4.3. Flutter analysis of the bridge at the 99% completion stage

In the coupled flutter analysis of the bridge with 99% completion, the first 30 natural modes computed in section 3.0 were employed as the participating modes. After the 3D characteristic equation for the flutter analysis of the bridge at 99% completion was established in the state-space format based on the information mentioned in section 4.1, the automatic searching method using the reduced frequency as a single searching parameter was applied to find the lowest critical wind speed. The lowest critical wind speed for the bridge at 99% completion was computed to be 245.2 m/s at a reduced velocity of 12.55 and a flutter frequency of 0.367 Hz (see Table 5).

Figs. 6(a) to 6(c) show the distribution of relative modal amplitude, modal energy ratio, modal phase angle over the 30 participating modes of vibration, respectively. It is noted that vibration mode 3 (first deck vertical mode), mode 4 (second deck vertical mode), mode 5 (third deck vertical mode), and mode 7 (first deck torsional mode) are the four major participating modes dominating

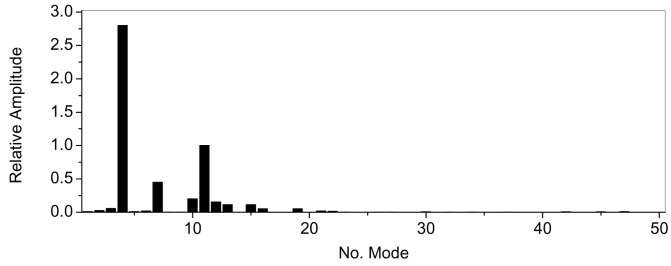

(a) Relative modal amplitude at the lowest critical wind speed

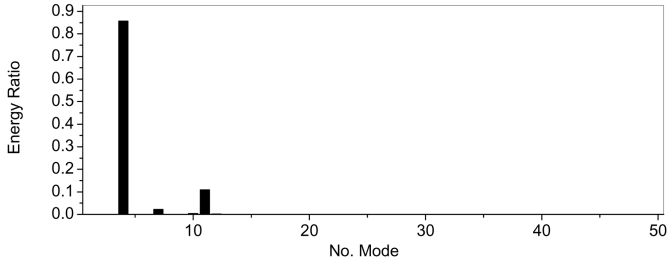

(b) Modal energy ratio at the lowest critical wind speed

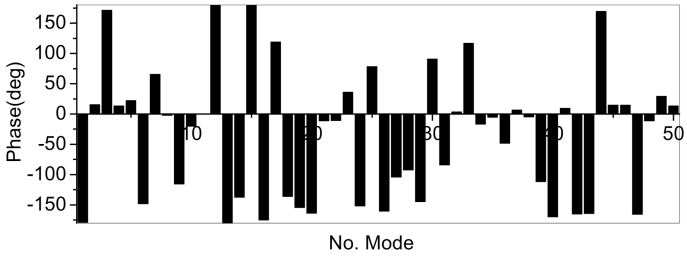

(c) Modal phase angle at the lowest critical wind speed

Fig. 4 Modal information of the completed bridge at the lowest critical wind speed

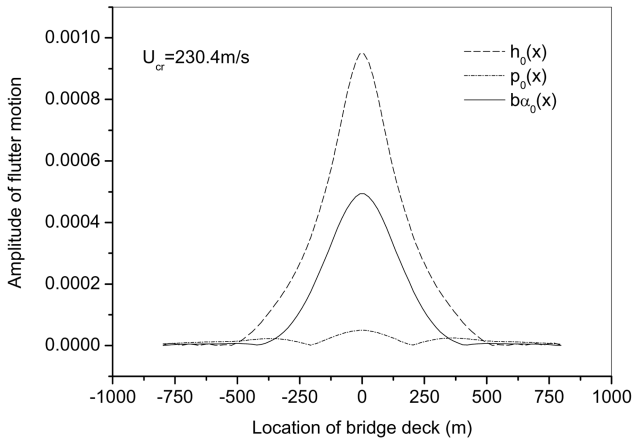

Fig. 5 Relative amplitudes of deck motion along the bridge longitudinal axis at 100% completion

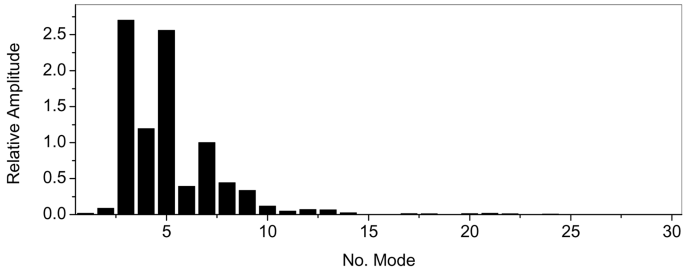

(a) Relative modal amplitude at the lowest critical wind speed

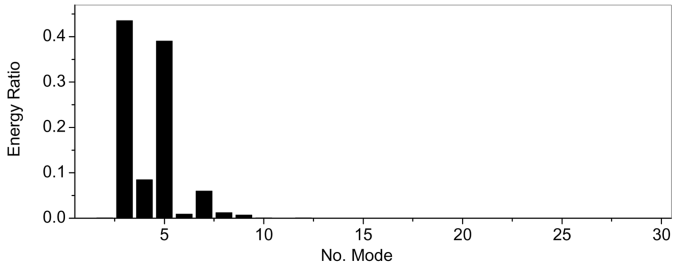

(b) Modal energy ratio at the lowest critical wind speed

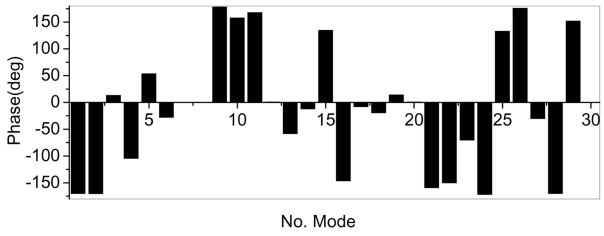

(c) Modal phase angle at the lowest critical wind speed

Fig. 6 Modal information of the bridge at 99% completion at the lowest critical wind speed

the flutter instability of the bridge at 99% completion. The phase angles of the four major participating modes are different. It is also noted that the mode 6 (fourth deck vertical mode), mode 8 (deck torsional mode) and mode 9 (deck torsional mode) also make small contributions to the flutter instability of the bridge at 99% completion.

Fig. 7 shows the relative amplitudes of the vertical, lateral, and torsional displacement responses (flutter motion) of the bridge deck along the bridge longitudinal axis at the lowest critical wind speed. It is noted that again the vertical vibration and torsional vibration dominate the flutter motion of the bridge deck at this construction stage.

4.4. Flutter analysis of the bridge at the 82% completion stage

In the coupled flutter analysis of the bridge at 82% completion, the first 30 natural modes computed in section 3.0 were employed as the participating modes. After the 3D characteristic equation for the flutter analysis of the bridge at 82% completion is established in the state-space

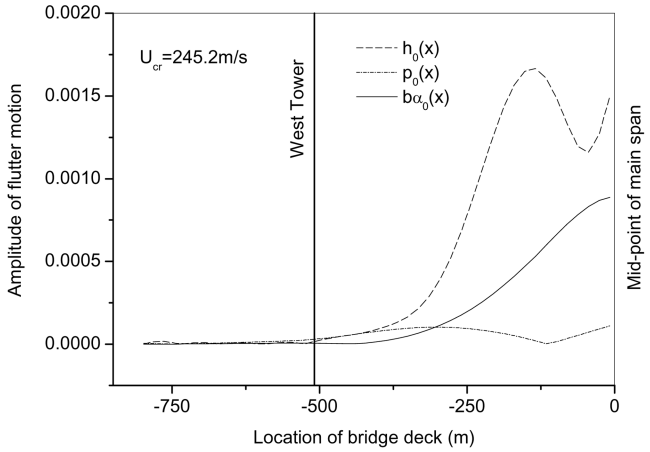

Fig. 7 Relative amplitudes of deck motion along the bridge longitudinal axis for the bridge at 99% completion

format based on the information mentioned in section 4.1, the automatic searching method using the reduced frequency as a single searching parameter is applied to find the lowest critical wind speed. The lowest critical wind speed for the bridge at 82% completion was computed to be 306.0 m/s at a reduced velocity of 13.42 and a flutter frequency of 0.428 Hz (see Table 5).

Figs. 8(a) to 8(c) show the distribution of relative modal amplitude, modal energy ratio, modal phase angle over the 30 participating modes of vibration, respectively. It is noted that vibration mode 3 (first deck vertical mode), mode 4 (deck vertical mode and tower longitudinal mode), mode 5 (deck vertical mode), and mode 7 (first deck torsional mode) are the four major participating modes dominating the flutter instability of the bridge at 82% completion. The phase angles of the four major participating modes are different. It is also noted that the mode 8 (deck vertical mode) and mode 9 (deck torsional mode) also make small contributions to the flutter instability of the bridge with 82% completion.

Fig. 9 shows the relative amplitudes of the vertical, lateral, and torsional displacement responses (flutter motion) of the bridge deck along the bridge longitudinal axis at the lowest critical wind speed. It is noted that again the vertical vibration and torsional vibration dominate the flutter motion of the bridge deck at this construction stage.

4.5. Flutter analysis of the bridge at the 61% completion stage

In the coupled flutter analysis of the bridge at 61% completion, the first 30 natural modes computed in section 3.0 are employed as the participating modes. After the 3D characteristic equation for the flutter analysis of the bridge at 61% completion was established in the state-space format based on the information mentioned in section 4.1, the automatic searching method using the reduced frequency as a single searching parameter was applied to find the lowest critical wind speed. The lowest critical wind speed for the bridge at 61% completion is computed to be 407.7 m/s at a reduced velocity of 14.99 and a flutter frequency of 0.510 Hz (see Table 5).

Figs. 10(a) to 10(c) show the distribution of relative modal amplitude, modal energy ratio, modal phase angle over the 30 participating modes of vibration, respectively. It is noted that vibration mode 3 (first deck vertical mode), mode 4 (deck vertical mode and tower longitudinal mode), mode

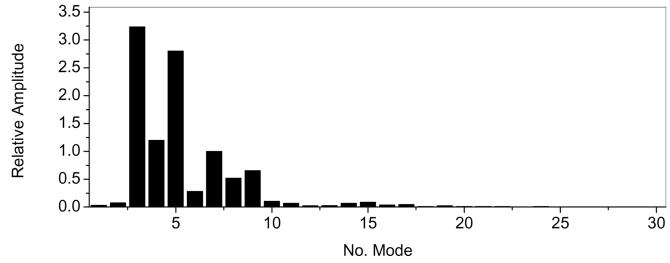

(a) Relative modal amplitude at the lowest critical wind speed

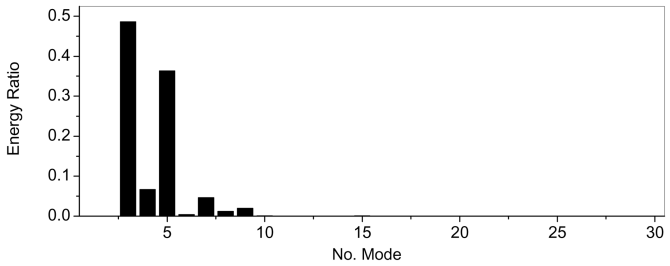

(b) Modal energy ratio at the lowest critical wind speed

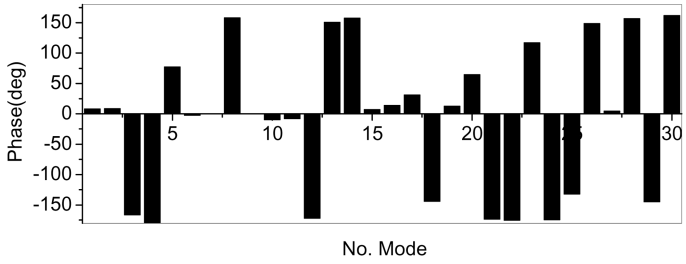

(c) Modal phase angle at the lowest critical wind speed

Fig. 8 Modal information of the bridge at 82% completion at the lowest critical wind speed

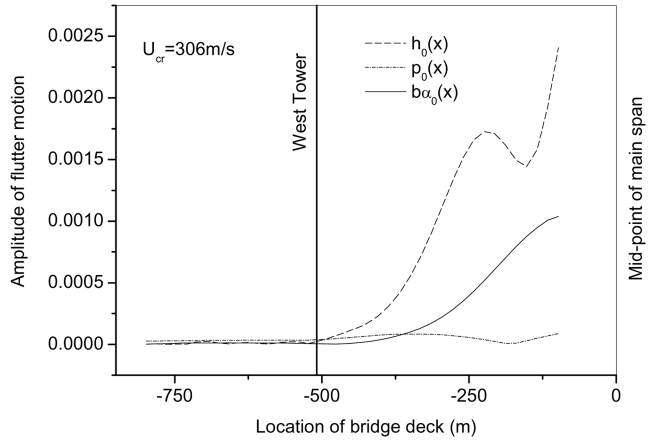

Fig. 9 Relative amplitudes of deck motion along the bridge longitudinal axis for the bridge at 82% completion

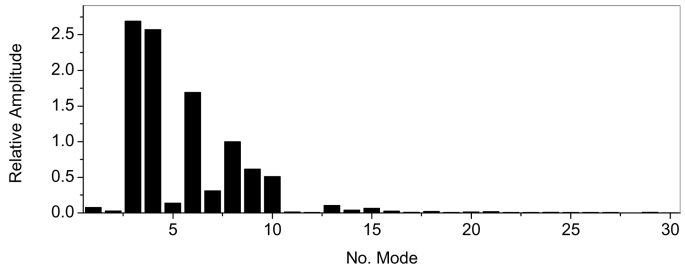

(a) Relative modal amplitude at the lowest critical wind speed

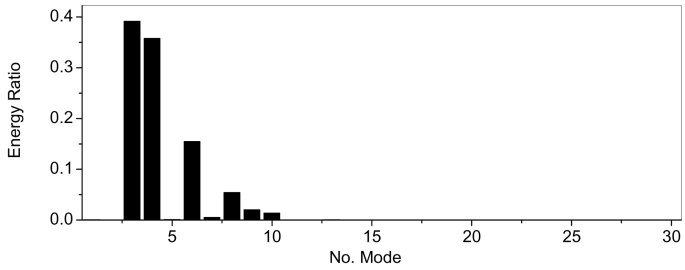

(b) Modal energy ratio at the lowest critical wind speed

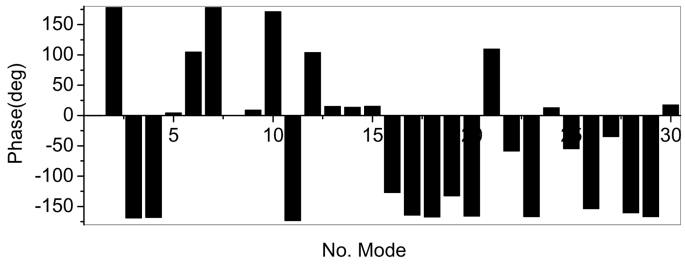

(c) Modal phase angle at the lowest critical wind speed

Fig. 10 Modal information of the bridge at 61% completion at the lowest critical wind speed

6 (deck vertical mode), and mode 8 (first deck torsional mode) are the four major participating modes dominating the flutter instability of the bridge at 61% completion. The phase angles the mode 3 and mode 4 are very much similar but are different from the other participating mode 6 and mode 8. It is also noted that the mode 9 (tower longitudinal mode) and mode 10 (deck vertical mode) also make small contributions to the flutter instability of the bridge at 61% completion.

Fig. 11 shows the relative amplitudes of the vertical, lateral, and torsional displacement responses (flutter motion) of the bridge deck along the bridge longitudinal axis at the lowest critical wind speed. It is noted that again the vertical vibration and torsional vibration dominate the flutter motion of the bridge deck at this construction stage.

4.6. Flutter analysis of the bridge at the 39% and 22% completion stage

Flutter analyses of the Bridge at the 39% and 22% completion stage indicated the critical wind

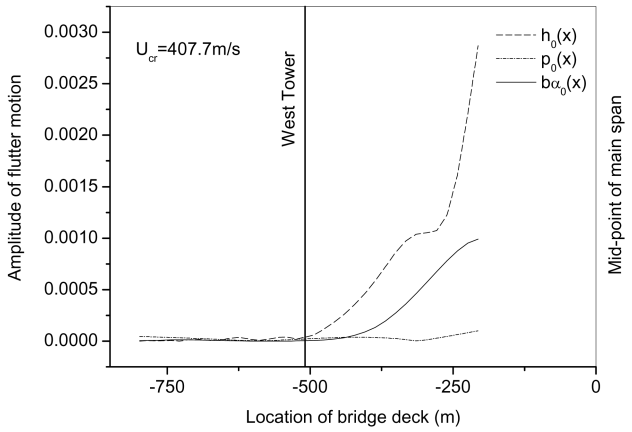

Fig. 11 Relative amplitudes of deck motion along the bridge longitudinal axis for the bridge at 61% completion

speeds occur at a reduced velocity of 13.50 (flutter frequency = 0.758 Hz) and 13.99 (flutter frequency = 1.005 Hz) respectively, leading to even higher critical wind speeds than that associated with 61% completion.

5. Conclusions

The 3-D finite element based coupled flutter analysis has been performed in this study to evaluate the critical flutter wind speeds of Stonecutters Bridge at its in-service stage as well as the various construction stages. The analyses confirm that the aerodynamic twin-deck girder design for Stonecutters Bridge will make the bridge extremely stable against divergent oscillation of flutter at various stages of its life. 6 finite element models and hence 6 sets of dynamic characteristics were established covering the 6 stages of the bridge under investigation. The single parameter searching method developed by the second author of this paper was found to be very efficient in identifying not just the critical flutter wind speeds, but also the dominant modes of vibration participating in the vibration as well as the relative phase angles of individual modes under consideration.

The computed lowest critical wind speeds of the completed bridge and the bridge with 22%, 39%, 61%, 82%, and 99% completion ratios are all listed in Table 5 together with the corresponding reduced velocities and flutter frequencies. The flutter analyses performed clearly demonstrate that

Table 5 Lowest critical flutter wind speed for Stonecutters Bridge

Model		Flutter velocity U_{cr} (m/s)	Reduced velocity (U/fB)	Flutter frequency (Hz)
Construction stage	Ratio=22%	Much higher than 407.7 m/s	13.99	1.005
	Ratio=39%		13.50	0.758
	Ratio=61%	407.7	14.99	0.510
	Ratio=82%	306.0	13.42	0.428
	Ratio=99%	245.2	12.55	0.367
Completion stage		230.4	13.08	0.331

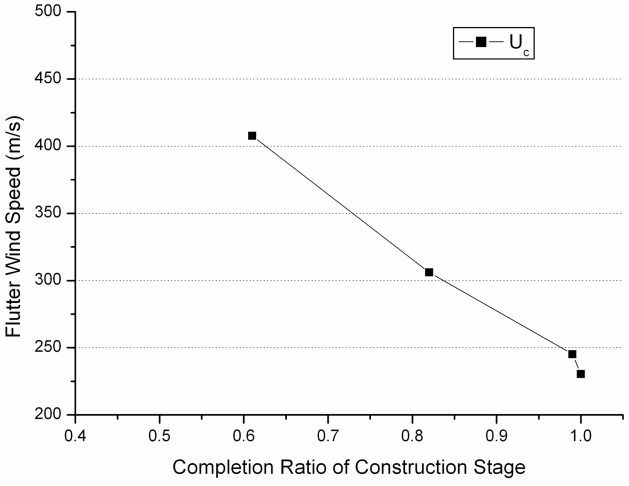

Fig. 12 Variation of critical flutter wind speeds for Stonecutters Bridge against completion ratio

the vertical and torsional modes of vibration of the bridge deck dominate the flutter instability of the bridge, and the multi-modes of vibration other than single mode of vibration are involved in the flutter instability of the bridge at both the completion stage as well as the construction stage. The lowest critical wind speed of the bridge as a function of completion ratio is plotted in Fig. 12. It is seen that the lowest critical wind speed of the bridge decreases with increasing completion ratio with the globally lowest critical wind speed being 230.4 m/s at the completion stage of the bridge. Such a high wind speed would unlikely occur in reality, and thus the computed critical wind speeds are of theoretical interest only and indicate no flutter instability problems for Stonecutters Bridge.

Acknowledgements

The authors wish to express their gratitude to the Director of Highways of the HKSAR, Ir CK Mak, for his permission to publish this paper. Views expressed in the paper are entirely those of the authors.

References

Agar, T. A. (1989), "Aerodynamic flutter analysis of suspension bridges by a modal technique", *Eng. Struct*., 75-82.

Bleich, F. (1948), "Dynamic instability of truss-stiffened suspension bridges under wind action", *Proc. ASCE*, **74**(7), 1269-1314.

Boonyapinyo, V., Miyata, T., and Yamada, H., *et al*. (1999), "Advanced aerodynamic analysis of suspension bridges by state-space approach", *J. Struct. Eng.*, ASCE, **125**(12), 1357-1366.

Chen, X., Matsumoto, M., and Kareem, A. (2000a), "Aerodynamic coupling effects on flutter and buffeting of bridges", *J. Eng. Mech*., ASCE, **126**(1), 17-26.

Chen, X., Matsumoto, M., and Kareem, A. (2000b), "Time domain flutter and buffeting response analysis of bridges", *J. Eng. Mech*., ASCE, **126**(1), 7-16.

Chen, X. and Kareem, A. (2003), "New frontiers in aerodynamic tailoring of long span bridges: and advanced analysis framework", *J. Wind Eng. Ind. Aerodyn*., **91**(12-15), 1511-1528.

Chen, Z.Q. (1994), "The three dimensional analysis and behaviors investigation on the critical flutter state of bridges", *Proc. Symp. on Cable-stayed bridges*, Shanghai, China.
Diana, G., Cheli, F., Zasso, A., and Bocciolone, M. (1999), "Suspension bridge response to turbulent wind: Comparison of new numerical simulation method results with full scale data", *Wind Engineering into the 21 Century,* A. Larsen, G.L. Larose and F. M. Livesey (eds), Balkema, Rotterdam, The Netherlands, 871-878.
Ding, Q.S., Chen, A.R., and Xiang, H.F. (2002), "A state space method for coupled flutter analysis of long-span bridges", *Struct. Eng. Mech.*, **14**(4), 491-504.
DMI (2001), "Section Model Tests for Stonecutters Bridge", Hong Kong, AJ Section, DMI Report 2001197, Nov 2001.
Dung, N. N., Miyata, T., and Yamada, H., *et al*. (1998), "Flutter responses in long span bridges with wind induced displacement by the mode tracing method", *J. Wind. Eng. Ind. Aerodyn.*, **78&79**, 367-379.
Ge, Y. J. and Tanaka, H. (2000), "Aerodynamic flutter analysis of cable-supported bridges by multi-mode and full-mode approaches", *J. Wind Eng. Ind. Aerodyn.*, **86**, 123-153.
Jain, A., Jones, N.P., and Scanlan, R.H. (1996), "Coupled flutter and buffeting analysis of long-span bridges", *J. Struct. Eng.,* ASCE, **122**(7), 716-725.
Lin, Y.K., "Motion of suspension bridges in turbulent wind", *J. Eng. Mech. Div.,* ASCE, **105**(6), 1979.
Matsumoto, M., Shijo, R., and Eguchi, A., *et al*. (2004), "On the flutter characteristics of separated two box girders", *Wind and Struct.*, **7**(4), 281-291.
Miyata, T. and Yamada, H. (1988), "Coupled flutter estimate of a suspension bridge", *Proc. Int. Colloquium on Bluff Body Aerodyn. and Its Appl.*, Kyoto, 485-492.
Miyata, T., *et al*. (1994), "New findings of coupled flutter in full model wind tunnel tests on the Akashi Kaiko Bridge", *Proc. Symp. on Cable-stayed and Suspension Bridges*, Deauvlille, France, 163-170.
Namini, A. and Albrecht, P. (1992), "Finite element-based flutter analysis of cable-suspended bridges", *J. Struct. Eng.,* ASCE, **118**(6), 1509-1526.
Ogawa, K., Shimodoi, H., and Oryu, T. (2002), "Aerodynamic characteristics of a 2-box girder section adaptable for a super-long span suspension bridge", *J. Wind Eng. Ind. Aerodyn.*, **90**(12-15), 2033-2043.
Sato, H., Kusuhara, S., Ogi, K., *et al*. (2000), "Aerodynamic characteristics of super long-span bridges with slotted box girder", *J. Wind Eng. Ind. Aerodyn.*, **88**(2-3), 297-306.
Scanlan, R.H. (1978), "The action of flexible bridges under wind, I: flutter theory," *J. Sound Vib.*, **60**(2), 187-199.
Scanlan, R.H. and Lin, W. (1987), "Effects of turbulence on bridge flutter derivatives", *J. Eng. Mech. Div.,* ASCE, **104**(4), 719-733.
Scanlan, R.H. and Jones, N.P. (1990), "Aeroelastic analysis of cable-stayed bridges", *J. Struct. Eng.*, ASCE, **116**(2), 229-297.
Scanlan, R.H. (1993), "Problematic in formulation of wind-force model for bridge decks", *J. Struct. Eng.*, ASCE, **119**(7), 1433-1446.
Xiang, H., *et al*. (1996), "Investigations on the wind-resisted behavior of Jiangyin Yangtse Suspension Bridge", *Bulletin of Laboratory of Wind tunnel, SKLDRCE, Tongji Univ.*, Shanghai, China. (in Chinese).
Xie, J. and Xiang, H. (1985), "State-space method for 3-D flutter analysis of bridge structures", *Proc. Asia Pacific Symp. on Wind Eng.*, India, 269-276.

CC